doi: 10.2965/jwet.18-081 Journal of Water and Environment Technology, Vol.17, No.3: 180–193, 2019

Original Article

Biosorption of Fe (II) from Aqueous Solution by Brewing Waste: Equilibrium and Kinetic Studies

Enoch Akinbiyi Akinpelu, Elvis Fosso-Kankeu, Frans Waander

Water Pollution Monitoring and Remediation Initiatives Research Group, School of Chemical and Minerals Engineering, North-West University, Potchefstroom, South Africa

ABSTRACT

The physicochemical analysis of surface water of Mooi and Vaal rivers network indicated that the concentration of iron was far above the required limit by the South Africa water regulation. In this study, brewing waste was used as biosorbent for the removal of iron from synthetic solution to develop strategies for remediation of Mooi and Vaal rivers network pollution. X-ray diffraction (XRD), Fourier-transform infrared spectroscopy (FTIR) and scanning electron microscope (SEM), were used for the characterisation of the sorbent. BET was calculated using nitrogen and carbon dioxide adsorption data. Batch tests were conducted to evaluate the influence of sorbent concentration and pre-treatment on the iron removal. The brewing waste showed a removal percentage of 93% with residual iron concentration of 2.6 mg L^{-1} while the acid pre-treated brewing waste indicated 98% removal and 0.6 mg L^{-1} residual iron concentration. The adsorption equilibrium, based on correlation coefficients, was best described by Dubinin-Radushkevich and Langmuir, for raw and acid pre-treated brewing waste, respectively. The kinetic data were best described by pseudo-first-order with correlation coefficients (R^2) of 0.9898 and 0.9968 for both raw and acid pre-treated brewing waste, respectively. The mass transfer coefficient indicates the intraparticle diffusion controls the rate of sorption of iron in this study.

Keywords: biosorption, brewing waste, equilibrium, iron, kinetic modelling

INTRODUCTION

The increasing rate of industrialisation in many developing countries has led to diverse challenges in water management particularly in mineral processing industry. Since the inception of 21st century, communities have started experiencing water crisis due to poor water management, population growth and industrialisation. Mining activity is responsible for most of the toxic industrial wastewater due to direct discharge of partially treated wastewater into fresh water bodies, and could leach into the water table thereby contaminating the groundwater. Hence, the need for proper treatment of wastewater before it is discharged into the environment. This will protect the environment and secures public health.

South Africa is well known for its abundance of mineral resources. It is considered as the 5th largest mining sector in terms of its Gross Domestic Product (GDP) contribution [1]. A recent study on the surface water in the vicinity of Potchefstroom, South Africa showed the proliferation of diverse contaminants above the government required limit [2]. The concentration of iron was found to be 36 mg L^{-1} contrary to the South African national standard for drinking water [3] –2.0 mg L^{-1} and guidelines for drinking water quality by World Health Organisation [4] –0.1 mg L^{-1}. This high concentration of iron in the surface water makes it unfit for both human and animal consumption.

Several conventional methods for removal of pollutants from water includes sedimentation, coagulation and flocculation, ion-exchange, filtration, membrane filtration and reverse osmosis, amongst other technologies [5,6]. However, these methods often generate large amount of waste products that requires further treatment before disposal, high energy consumption, including cost implication when treating large volume of wastewater containing low concentrations of pol-

Corresponding author: Enoch A. Akinpelu, E-mail: biyipelu@gmail.com
Received: August 26, 2018, Accepted: January 10, 2019, Published online: June 10, 2019

lutants make them unsuitable on a large scale [7]. Biosorption has been shown as a potential alternative to the conventional methods of removing heavy metals from wastewater due to its robustness and environmental benignity [8]. Biological materials are known to have affinity for heavy metals owing to their metal binding capacities [7]. Thus, the application of food industry residues like sorghum beer processing waste; which is available in large volume is a promising biosorbent for the removal of heavy metals such as iron. Generally, brewing waste consists of cell wall debris, plumule, malt bark, coagulated protein, including high fibre content which are often use for animal nutrition [9]. In South Africa, sorghum beer industry has experienced significant increase in participation especially in the last decade resulting in major rise of the residue [10]. The availability of these brewing waste in South Africa could therefore provide a potential low cost solution for the treatment of polluted water.

Therefore, the objective of this study was to investigate the sorption capacity of sorghum brewing waste for the removal of iron from synthetic solution prepared based on the results from the physicochemical analysis of the surface water in the vicinity of Potchefstroom. X-ray Diffraction (XRD), Fourier-transform infrared spectroscopy (FTIR) and scanning electron microscopy (SEM), as well as nitrogen and carbon dioxide, Brunauer-Emmett-Teller (BET) surface area analyses were used for the characterisation of the sorbent.

MATERIALS AND METHODS

Chemicals and reagents

Iron (II) sulphate heptahydrate ($FeSO_4.7H_2O$, ≥98.0%) was used for preparation of 40 mg Fe^{2+} L^{-1}, in distilled water. This solution was designated work-solution. The work-solution pH was adjusted using 1 mol L^{-1} HCl and 1 mol L^{-1} NaOH. All reagents were of analytical grade and were purchased from Sigma-Aldrich (Modderfontein, South Africa).

Preparation and characterisation of biosorbent

Sorghum brewing waste (BW) was collected in a nearby brewing in Potchefstroom, South Africa. The High Performance Liquid Chromatography (HPLC) analysis of the BW showed that the waste is composed of hydrocarbon (6.27%), fat (1.58%) and protein (0.41%). The BW was washed in tap water in batch mode several times with constant manual stirring to remove possible impurities. Afterwards, the BW was washed with distilled water three times in batch mode and dried in an oven at 80˚C for 24 h to remove excess water. Half of the BW was pre-treated by 2 mol L^{-1} H_2SO_4 in order to remove sugars and protein from the structure and possibly increase the surface area of the biomaterial. This pre-treated BW was denoted PBW. The dried samples were pulverised into particle size between 0.85 to 1.18 mm prior to usage.

The Brunauer-Emmett-Teller (BET) surface area and pore size distribution of the samples were calculated using the nitrogen and carbon dioxide adsorption isotherm for mesopores and micropores measurement, respectively on a Micromeritics ASAP 2020 surface area and porosity analyser using a previously described approach, except that the samples were degassed under vacuum at 60˚C for 48 hours [11]. The density measurements were done in a Quantachrome Stereopycnometer, using helium gas at an outlet pressure of 134 kPa in a 10 cm^3 sample cell. Before actual measurement, samples were dried in oven at 105˚C for 12 h for complete removal of moisture and any volatile compounds. The surface structure and morphology were characterised by VEGA3 Scanning Electron Microscopy (TESCAN, Brno, The Czech Republic) at different magnifications. Cary 630 Fourier Transform Infrared Spectroscopy (FTIR) (Agilent Technologies, Santa Clara, USA) was used to determine the main functional groups present on the surface of the samples before and after the biosorption process, including the Supernova XRD (Agilent Technologies) examination, for structural and compositional changes in physical properties of the sorbent.

Biosorption experiments

Batch experiments were carried out in 250 mL Erlenmeyer flasks, where 50 mL of the work-solution was in contact with sorbents in mass ranging from 0.2 to 1.0 g (dry weight). After adding the sorbent, the pH was adjusted to 5 ± 0.2 using 1 mol L^{-1} HCl and 1 mol L^{-1} NaOH. The flasks were agitated for 2 h at 30 ± 0.2˚C on an orbital shaker at 150 rpm. After this, the solutions were filtered through 0.45 µm filter paper and the final pH was measured. The residual concentration of Fe (II) were quantified by inductively coupled plasma optical emission spectrometry (ICP-OES) (Agilent Technologies). All experiments were performed in triplicate. The batch kinetic experiments for the removal of Fe (II) were performed in three replicates. 500 mL Erlenmeyer flasks containing 200 mL work-solution and 1 g of sorbent. The flasks were agitated for 10 h at 30 ± 0.2˚C on a shaking incubator at 150 rpm. Samples were taken at intervals, filtered and analysed for the residual concentration of Fe (II) using ICP-OES. A blank sample without adsorbent was used as control in all cases.

Theory

The amount of metal sorbed per gram of sorbent and the percentage removal were estimated using the equations below:

$$q_e = (C_o - C_e)\frac{V}{m} \quad (1)$$

$$Removal(\%) = \frac{(C_o - C_e)}{C_o} \times 100 \quad (2)$$

where C_o and C_e are the metal ions concentrations in mg L^{-1} initially and at equilibrium, respectively, q_e is the equilibrium adsorption capacity (mg g^{-1}), m is the dry weight of biosorbent (g), and V is the work-solution volume (mL).

Sorption isotherm

Different isotherm models have been used to describe sorption equilibrium for wastewater treatment. Langmuir, Freundlich, Flory-Huggins, and Dubinin-Radushkevich isotherm models are being used for the present work.

Langmuir isotherm model

The Langmuir isotherm describes the monolayer adsorption onto a homogeneous surface without interaction between sorbed molecules [12]. The linear form of Langmuir isotherms is written as

$$\frac{C_e}{q_e} = \frac{C_e}{q_m} + \frac{1}{K_L q_m} \quad (3)$$

where q_m is the monolayer biosorption capacity on biosorbent (mg g^{-1}) and K_L is the Langmuir constant (L mg^{-1}). The values of K_L and q_m can be determined from linear plot of C_e/q_e and C_e. The Langmuir isotherm parameters can be used to predict the affinity of the sorbent for the sorbate using the dimensionless separation factor 'R_L' as expressed in the equation below [13].

$$R_L = \frac{1}{1 + K_L C_o} \quad (4)$$

The value of separation factor is between 0 and 1 for favourable adsorption while $R_L > 1$ represents unfavourable adsorption, $R_L = 1$ represents linear adsorption, and $R_L = 0$ represents irreversible adsorption process.

Freundlich isotherm model

The Freundlich isotherm describes sorption equilibrium on a heterogeneous surfaces and the linear form is represented as

$$\log q_e = \log K_F + \frac{1}{n}\log C_e \quad (5)$$

where n is the sorbtion intensity of the sorbent and K_F is the Freundlich constant. K_F and $1/n$ are evaluated from the intercept and slope of the plot of log qe versus log C_e, respectively.

Flory-Huggins isotherm model

The Flory-Huggins model is used to estimate the number of metal ions occupying sorption sites. The linear form is written as [14]:

$$\log \frac{\phi}{C_o} = \log K_{FH} + n \log(1 - \phi) \quad (6)$$

where $\phi = (1 - C_e / C_o)$ is the degree of coverage, n is the number of metal ions occupying sorption sites and K_{FH} is the Flory-Huggins constant. K_{FH} and n are determined from the intercept and slope of the plot of $\log \frac{\phi}{C_o}$ versus $\log(1 - \phi)$, respectively.

Dubinin-Radushkevich isotherm model

The Dubinin-Radushkevich (D-R) isotherm assumes the characteristics of the sorption curve is related to the porosity of the biosorbent. This model allows for the estimation of mean energy of sorption. The linear form is written as [15]:

$$\ln q_e = \ln Q_D - 2B_D RT \ln(1 + 1/C_e) \quad (7)$$

where Q_D is the maximum biosorption capacity (mol g^{-1}), B_D is the D-R model constant (kJ mol^{-1} K^{-1}), T is the absolute temperature (K) and R is the gas constant (kJ mol^{-1}). The value of B_D and Q_D is estimated from the slope and intercept of the plot ln q_e versus ln $(1+1/C_e)$, respectively. The mean energy of sorption E (kJ mol^{-1}) is evaluated from the relation [16]:

$$E = 1/\sqrt{2B_D} \quad (8)$$

Sorption kinetics

In order to predict the sorption kinetic models of Fe (II), pseudo-first-order and pseudo-second-order kinetic models were applied to the data.

Pseudo-first-order kinetic model

The linearised form of pseudo-first-order equation can be written as [17]:

$$\log(q_e - q_t) = \log(q_e) - \frac{k_1}{2.303}t \quad (9)$$

where q_t is the amount of metal uptake per mass of sorbent at any time (mg g^{-1}) and k_1 is the rate constant (min^{-1}) which can be calculated from the slope of the plot of log ($q_e = q_t$) versus time.

Pseudo-second-order kinetic model

The pseudo-second-order kinetic model is represented as follows [12,18]:

$$\frac{t}{q_t} = \frac{1}{k_2 q_e^2} + \frac{t}{q_e} \quad (10)$$

where $h = k_2 q_e^2$ is the initial sorption rate and k_2 is the rate constant. k_2 and h can be determined by plotting t/q_t against t.

Mass transfer analysis

The uptake of pollutant from the sorbate (liquid phase) to the sorbent (solid phase) is carried out by transfer of mass from former to the latter. According to the McKay et al model, three steps are involved in the sorption process, namely [19]:

1. Mass transfer of the sorbate from the liquid phase onto the solid surface;
2. Sorption of solute onto the surface sites; and
3. Internal diffusion of solute via either a pore diffusion model or homogeneous solid-phase diffusion model.

In this study, step (2) was assumed quick enough with respect to other steps and thus it is not rate limiting in the kinetic study. The McKay *et al.* (1981) [19] model equation (11) below was used for the mass transfer analysis.

$$\ln\left(\frac{C_t}{C_o} - \frac{1}{1+mK}\right) = \ln\left(\frac{mK}{1+mK}\right) - \left(\frac{1+mK}{mK}\right) \times \beta_L S_s t \quad (11)$$

where m is the mass of biosorbent per unit volume, $K = K_{Lqm}$ from Langmuir constant, β_L (cm s^{-1}) is the mass transfer coefficient and S_S (cm^{-1}) is the outer specific surface of the biosorbent particles per unit volume of the particle-free slurry. The value of β_L can be calculated from the slope of the plot of $\ln(C_t / C_o - 1/(1+mK))$ versus t (min). The S_S is calculated from the equation [19]:

$$S_s = \frac{6m}{d\,\rho(1-\varepsilon)} \quad (12)$$

where d is the diameter (cm), ρ is the density (g cm^{-3}) and ε is the porosity of the biosorbent.

Intraparticle diffusion model

During batch operation, there was possibility of transport of sorbate species into the pores of brewing waste, which is often the rate controlling step. Intraparticle diffusion plot can be used to identify the mechanism involved in the adsorption process. The intraparticle diffusion model is given by the equation [12]:

$$q_t = k_{id} t^{0.5} + C \quad (13)$$

where C is the intercept and k_{id} is the intraparticle diffusion rate constant (mg g^{-1} $min^{-0.5}$) estimated from the slope of plot q_t versus $t^{0.5}$.

Elovich kinetic equation

The Elovich equation is usually used to determine the kinetics of chemisorption of gases onto heterogeneous solids and lately, it has been used to describe the sorption of pollutants from aqueous solution [12,18]. The Elovich kinetic equation is written as:

$$\frac{dq_t}{dt} = \gamma\, exp(-aq_t) \quad (14)$$

where q_t is the sorption capacity at time t (mg g^{-1}), γ is the initial adsorption rate (mg g^{-1} min^{-1}) and a is the desorption constant. To simplify equation (14), it is assumed that $\gamma\, at \gg 1$. And by integrating and applying boundary conditions $q_t = 0$ *at* $t = 0$ *and* $q_t = q_t$ *at* $t = t$, equation (14) becomes

$$q_t = \gamma \ln(a\gamma) + \gamma \ln(t) \quad (15)$$

The plot of q_t versus ln(t) gives a straight line from which γ and a can be obtained from slope and interception, respectively.

Table 1 Physical characterisation of the biosorbent.

	Raw brewing waste (BW)	Pre-treated brewing waste (PBW)
Density (g cm^{-3})	1.22 ± 0.011	1.23 ± 0.024
N_2 adsorption		
BET surface area (m^2 g^{-1})	3.00×10^{-4}	1.88×10^{-2}
Total pore volume (cm^3 g^{-1})	1.82×10^{-4}	2.52×10^{-4}
CO_2 adsorption		
BET surface area (m^2 g^{-1})	188	76
Total pore volume (cm^3 g^{-1})	4.99×10^{-3}	4.68×10^{-3}

RESULTS AND DISCUSSION

Biosorbent characterisation

The pre-treatment resulted in increase in the density and mesopore surface area, including the pore volume of the sample as seen in **Table 1**. However, there was reduction in the micropore surface area. Generally, there are not many pores in brewing waste, which substantiate its low surface area as supported by previous findings [20,21]. **Figure 1** shows the micrographs of biosorbents with rough surfaces and few number of pores for both BW and PBW, before and after biosorption. The cross section shows irregular hole distributions in BW and PBW. **Figure 1C and D** show that the iron has occupied all the pores in both samples, including part of the rough surface of BW.

The FTIR spectra show the complex nature of brewing waste before and after biosorption process, a confirmation of several functional groups such as hydroxyl, amino and amide functional groups, including carboxyl; with potential to interact with metal ions (**Fig. 2**). The peak shows that the acid treatment results in changes in chemical structure of the brewing waste. It is observed that both spectra of BW and PBW have peaks at 1,278 and 1,651 cm^{-1} corresponding to the carbonyl group (C=O) stretching vibration in aldehydes, ethers, ketones and carboxylic acids, including the carbonyl group in aromatic rings found in lignin [22,23].

Also, peaks at 2,923.89 and 2,853.64 cm^{-1} conform to C-H stretching vibrations in aliphatic chains belonging to the cellulose, hemicellulose or lignin. The highest peak on both BW and PBW spectra was observed at 3,290.08 cm^{-1} which is typical of N-H (3,300–3,350 cm^{-1}) and H-O (3,200–3,600 cm^{-1}) stretching [24]. Notable difference in acid treatment causes displacement of peaks 1,098.78 and 723.10 cm^{-1} in BW by 1,095.39, 652.90 and 628.38 cm^{-1} in PBW. The latter peaks in PBW represent stretching vibration of S-O groups. After biosorption of iron, highest peak (3,290.08 cm^{-1}) in both BW and PBW disappeared. Also noticeable is the addition of peaks at 644.83, 614.58 and 607.58 cm^{-1} on BW spectra corresponding to S-O stretching vibration owing to the work-solution.

The X-ray diffraction patterns (**Fig. 3**) of BW and PBW before and after biosorption process show similar characteristic major peak from 15° to 35° 2θ, an indication of the presence of amorphous silica which agrees with previous report on brewing waste [25,26]. The acid treatment of brewing waste caused an increase in intensity and subsequent high percentage of silica as proposed in previous study [27]. Other components such as ethy-dimethylamino-methyl-carboxylate, benzo-alpha-pyrene, poly (ethylene terephthalate) and heneicosane, including *p*-diethylaminophenyl, were found to be significantly low. The XRD confirms the crystallinity of the iron on brewing waste.

Effect of biosorbent dosage

Several factors such as temperature, pH, initial metal ions concentration and biomass concentration; are known to affect the biosorption process. In order to mimic conditions in the surface water sample, temperature, pH and metal ion concentration in solution were kept constant, only the effect of biosorbent dosage on the biosorption process was examined and the results shown in **Fig. 4**. The increase in iron removal is proportional to the biosorbent dosage until it reaches 12 g L^{-1} of PBW. This performance can be attributed to higher mesopores surface area and accessibility of more active sites for sorption [20].

In addition, when biomass concentration is low, the metal ion can reach the cellular part, which in turns facilitate the metal ion concentration gradient [22]. Thus, an increase in biosorbent dosage decreases the amount of metal ion sorbed per unit mass (q), leading to the reduction in removal efficiency. However, for BW there was a steady increase in Fe (II) sorbed until it reached 16 g L^{-1} when it could no longer sorb the metal ion. The highest Fe (II) removal was 75% and 98% for BW and PBW, respectively. The lower removal

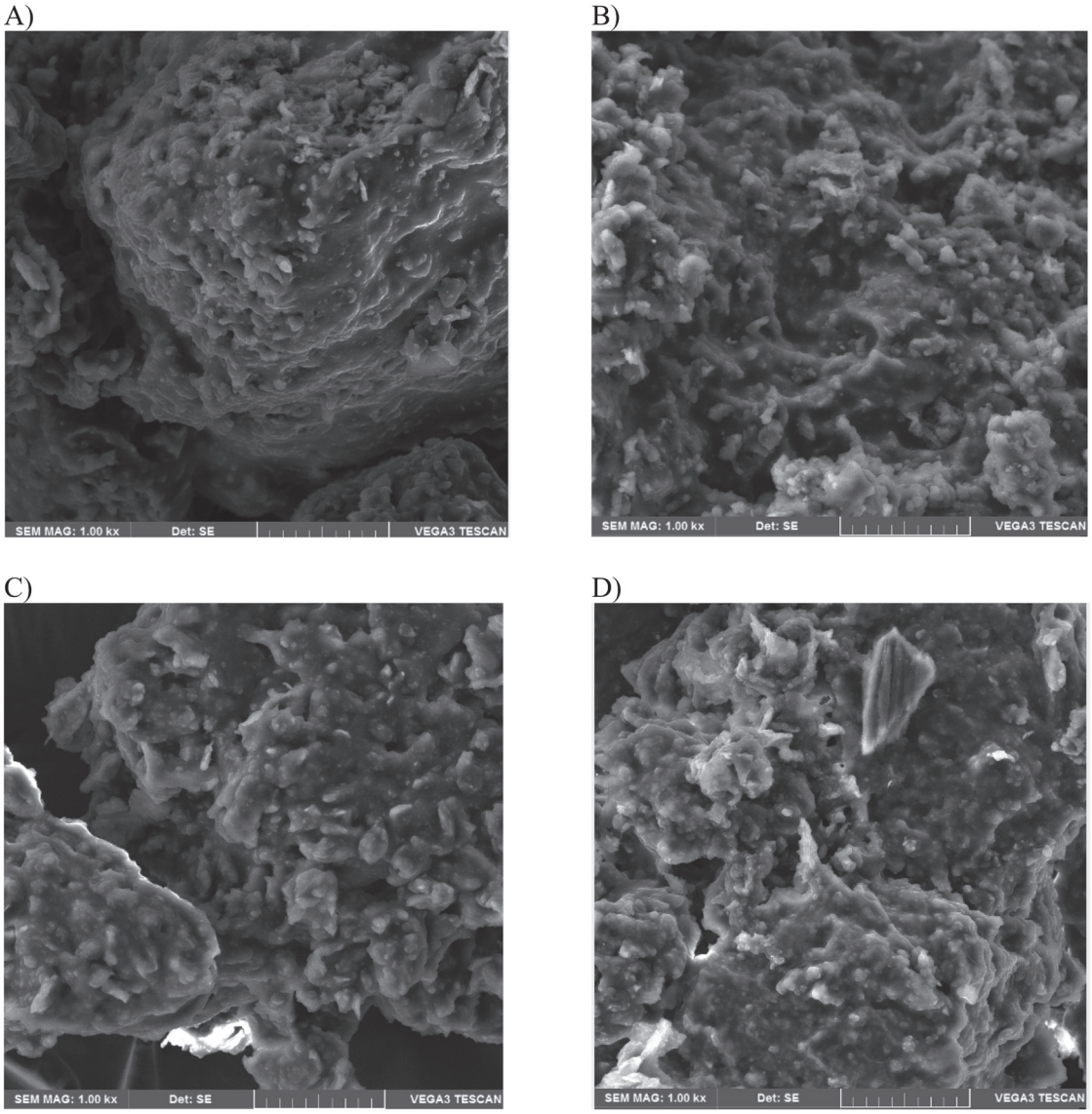

Fig. 1 Scanning electron micrograph image before adsorption; BW (A) and PBW (B) and after adsorption BW (C) and PBW (D).

efficiency in BW could be attributed to the lower surface area and higher biosorbent dosage. Comparatively, different efficiency of Fe (II) removal have been reported for several adsorbent. For instance, rice husk ash – 70% [28], maize cob – 48% [29], coconut coir fibre – 59% [30], dried biomass of activated sludge – 95% [31], cucumis melo rind – 98% [23]. Generally, the physical nature and pre-treatment method plays a major role in the variation of metal ion adsorbed. Furthermore, high biosorbent dosage are known to cause cell agglomeration and subsequent reduction in intercellular distance, which guarantees an excellent electrostatic interaction between the cells during biosorption [32]. Another factor of great importance in biosorption of metal ion is pH. The solution pH directly affect the competitive ability of hydrogen ions with metal ions for the active sites on the biosorbent surface [33]. It was observed that the decrease in pH is proportional to the increase in biosorbent dosage. At low pH, the adsorption of metal ion is low due to hydrogen ion competition and lower surface area of BW, thus the lower removal efficiency of Fe (II) at the later stage of the biosorption process [34,35].

Sorption isotherms

The adsorption isotherms parameters are shown in **Table 2**. The biosorption of Fe (II) in this study is well described by linear form of D-R isotherm model on BW with R^2 value

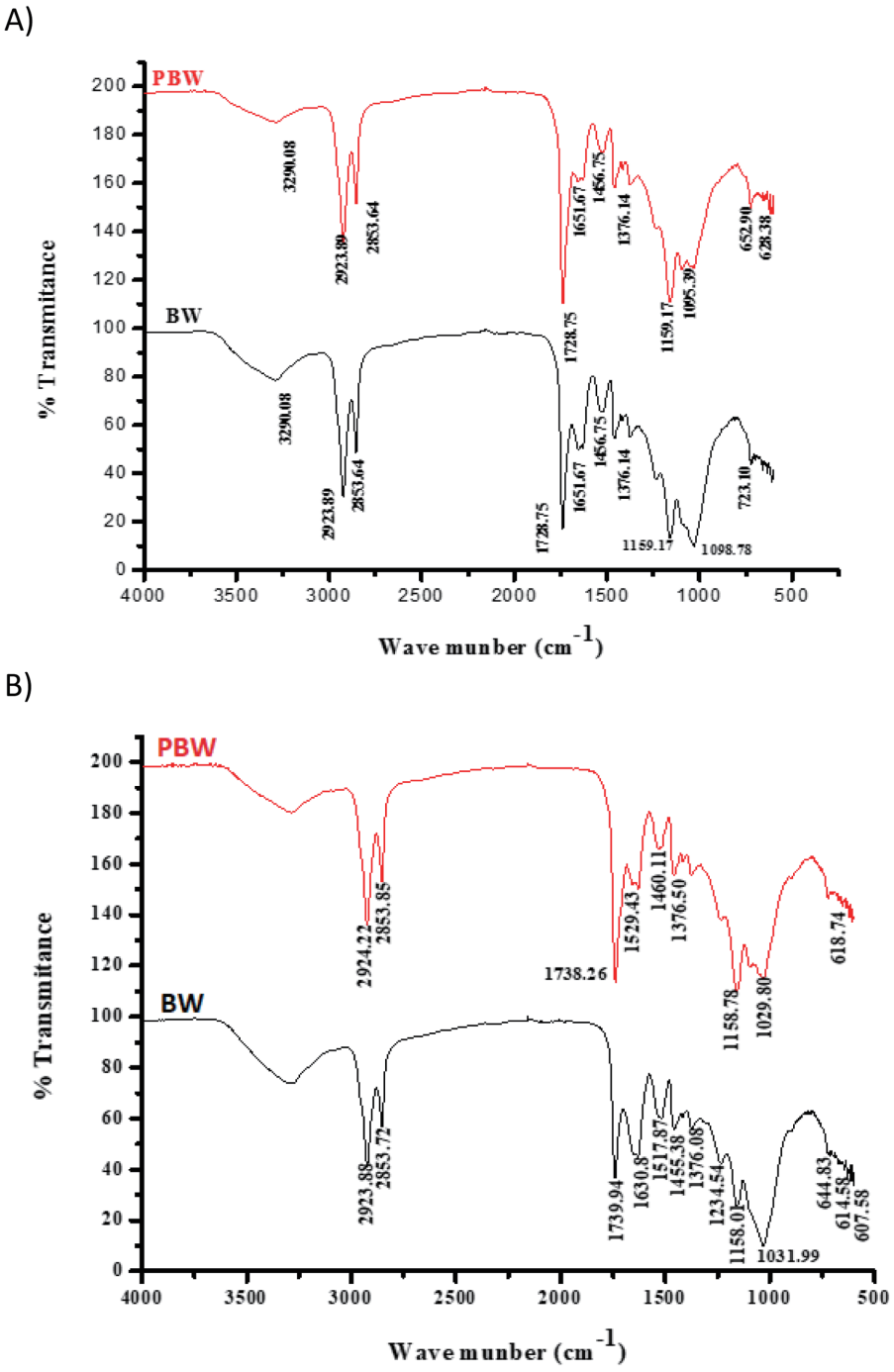

Fig. 2 FTIR spectra of brewing waste before (A) and after (B) adsorption of iron.

of 0.997 while linearised Langmuir isotherm model fitted well on PBW with R^2 value of 0.975, which supported the monolayer sorption. The Langmuir model is based on the assumptions that; (1) the adsorption is limited to the formation of a monolayer, (2) all binding sites possess an equal affinity for the adsorbate, (3) the number of adsorbed species does not exceed the total number of surface sites, and (4) there is a finite number of uniform adsorption between adsorbed species [36]. These assumptions may not be true for most complex systems involving biological materials. Nonetheless, the separation factor for both BW and PBW is between 0 and 1, which is an indication of a favourable biosorption process [34]. Also, **Table 2** shows that both BW and PBW have similar affinity for Fe (II) but BW has higher Fe (II)

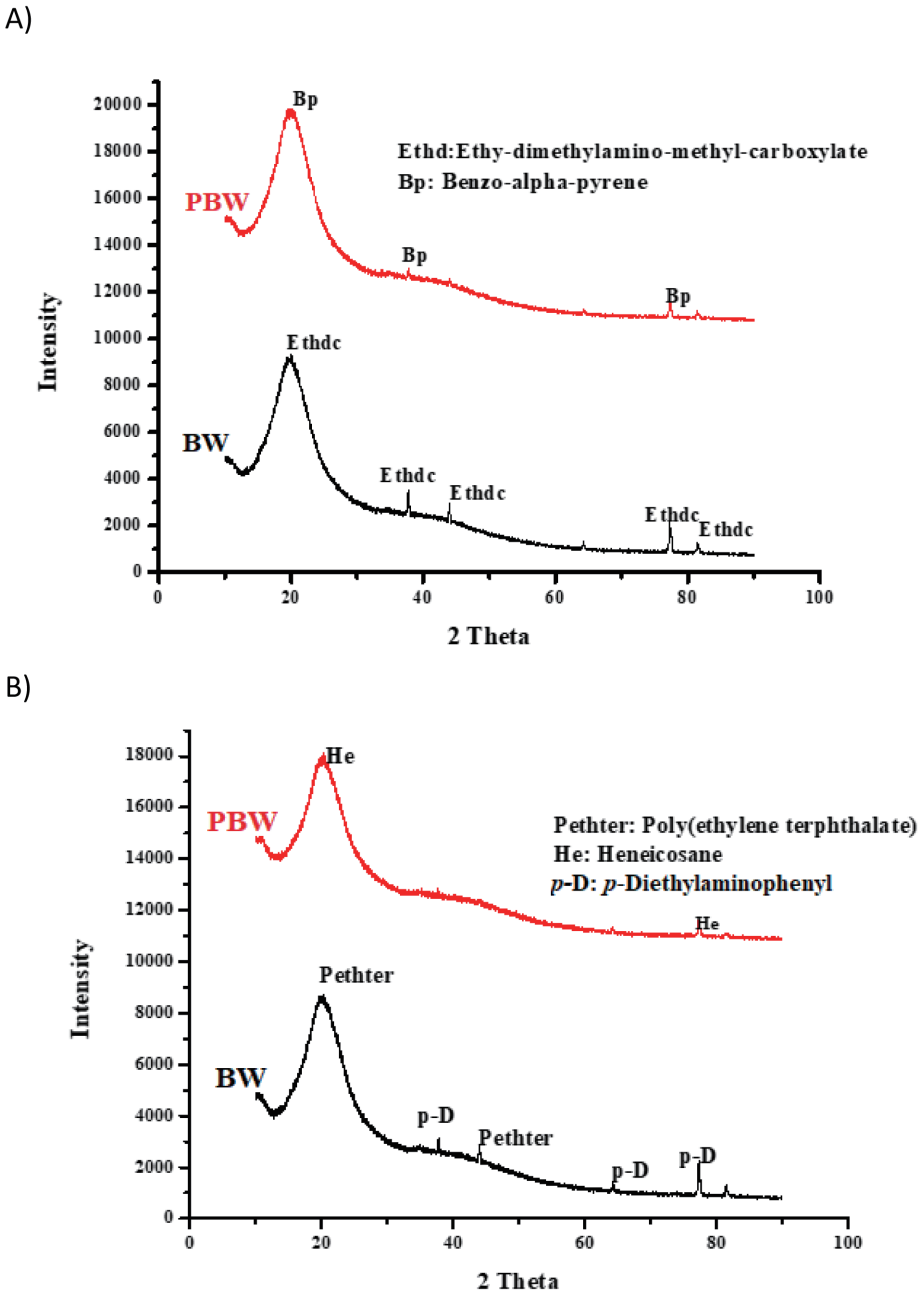

Fig. 3 XRD spectra of brewing waste before (A) and after (B) adsorption of iron.

maximum uptake capacity (q_m = 1.769 mg g^{-1}). The observed decrease in brewing metal uptake capacity resulting from acid pre-treatment could be as a result of structural and/or chemical changes interfering in quantity and availability of biosorbent biding sites. Meanwhile, acid pre-treatment of banana trunk fibers resulted in improved uptake of Fe(II) from 2.42 to 2.45 mg g^{-1} described by Freundlich isotherm model [37]. The Freundlich isotherm model is a demonstration of multilayer sorption process with an adsorption intensity (1/n) less than 1 for both BW and PBW, which suggests the physical adsorption of Fe (II) on the brewing waste [20,28]. In summary, both Langmuir and Freundlich models fitted well the experimental biosorption equilibrium data, similar to the earlier report of biosorption of Fe (II) on brewing waste [20]. The D-R model was included to elucidate the adsorption energy. The high Q_D in PBW indicates high sorption capacity compared with BW. The mean sorption energy E gives information about biosorption mechanism. If E < 8 kJ mol^{-1}, the biosorption process is physically driven, if E value is between 8 kJ mol^{-1}. and 16 kJ mol^{-1}., the biosorption process

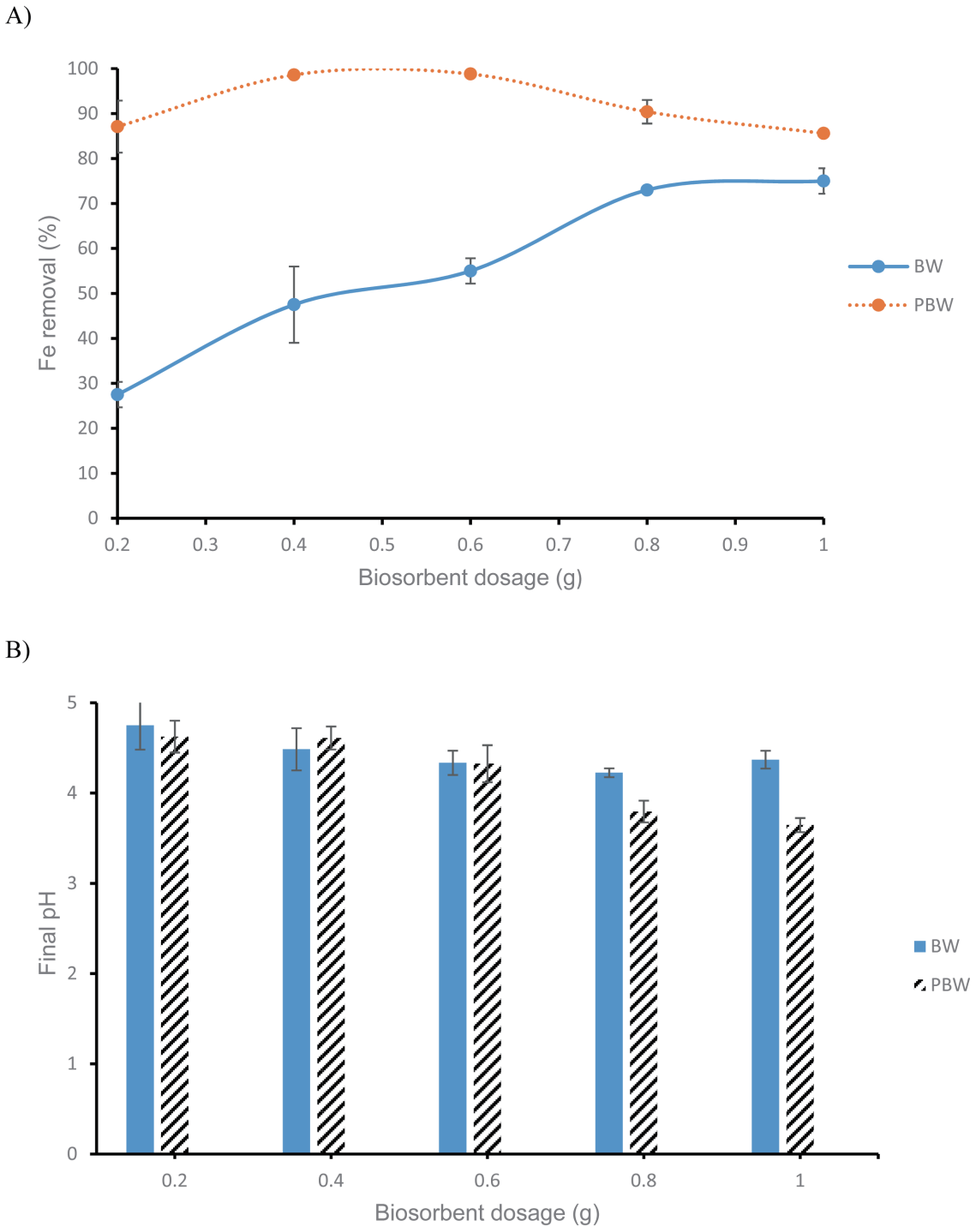

Fig. 4 Removal of iron for (A) different concentration of biosorbent; C_o = 40 mg L^{-1} and (B) final pH of the solution; $pH_{initial}$ = 5 ± 0.2.

is chemically driven, and if E > 16 kJ mol^{-1}., diffusion has more significance in the biosorption process [34]. The mean sorption energy for BW and PBW indicates diffusion is most prominent in the biosorption of Fe (II) on brewing waste.

Statistically, at 95% confidence level, the T test showed that there was no significant difference between the experimental data and model parameters of Langmuir and Freundlich, although the R^2 values differ for both BW and PBW. Meanwhile, experimental data of Flory-Huggins and Dubinin-Radushkevich models, fitted best on BW with deviation of

Table 2 Coefficients of isotherm models for iron removal. [Contact time = 10 h, pH = 5±0.2, 30 ˚C, 150 rpm]

Isotherm parameters	Biosorbents	
	BW	PBW
Langmuir		
q_m	1.77	1.19
K_L	0.134	0.109
R_L	0.157	0.186
R^2	0.977	0.975
Freundlich		
$1/n$	0.579	0.472
K_F	15.5	10
R^2	0.989	0.971
Flory-Huggins		
n	0.558	0.364
K_{FH}	164	144
R^2	0.981	0.846
Dubinin-Radushkevich		
Q_D	2.36	3.09
B_D	7.69×10^{-4}	2.13×10^{-4}
E	25.5	48.5
R^2	0.997	0.830

2.2% and 1.6%, respectively. IBM Statistical Package for the Social Sciences (SPSS) software v24.0 was deployed for the statistical analyses.

Biosorption kinetics

Figure 5 shows the removal of Fe (II) over time by 5 g L^{-1} brewing waste. The Fe (II) removal increases steadily in the first few hours, reaching equilibrium at about 240 min of contact with BW and increased rapidly in the last 200 min of contact to a maximum removal of 93% of Fe (II). In the case of PBW, there was rapid increase in Fe (II) sorption at the initial stage up to 90 min until it reached equilibrium at approximately 120 min but became slow at the later stage until it attained maximum removal of 98% of Fe (II). Different equilibrium time have been reported for different biological materials for the removal of Fe (II) from aqueous solutions. Equilibration time of 120, 45, 60, 150 and 360 minutes were reported for removal of Fe (II) using rice husk ash, cucumis melo rind, orange peel, dried biomass of activated sludge and chitosan, respectively [23,28,31,34,38]. The higher adsorption rate in PBW could be due to the higher number of active sites at the beginning as shown by BET characterisation in **Table 1**. Statistically, there were no significant difference ($p<0.05$) between the sorption by BW and PBW.

The values of the model parameters for the pseudo-first-order and pseudo-second-order kinetics modelling of Fe (II) biosorption on BW and PBW are presented in **Table 3**. It was observed that the acid pre-treated brewing waste (PBW) ($R^2 = 0.997$) gave a better fit than raw brewing waste (BW) ($R^2 = 0.990$) in pseudo-first-order while BW ($R^2 = 0.966$) is better fitted in pseudo-second-order than PBW ($R^2 = 0.936$). In both cases, rate constants (k_1 and k_2) were calculated from the linearised form of their respective equations (9) and (10). From pseudo-second-order, it could be assumed that the rate limiting step of Fe (II) unto brewing waste is chemisorption. Equilibrium concentration of Fe (II) predicted by pseudo-second-order kinetic model agrees well with the experimental value for PBW (q_{exp} = 7.8 mg g^{-1}) than BW (q_{exp} = 7.4 mg g^{-1}). Fontana *et al*. (2018) [20] had earlier reported similar trend on Fe (II) adsorption on brewing waste with high correlation coefficients on both pseudo-first-order and pseudo-second-order, which further confirms the potential of this industrial waste for Fe (II) biosorption [31].

The constants γ (initial sorption rate) and a (desorption capacity) obtained from slope and intercept of the linearised Elovich equation plot for Fe (II) sorption on for BW and PBW is shown in **Table 3**. The model fits fairly well with the experimental data with a better correlation coefficient (R^2 = 0.881) and initial sorption rate (γ = 2.6 mg g^{-1} min^{-1}) for PBW. This good fit has been confirmed in study by [31] and

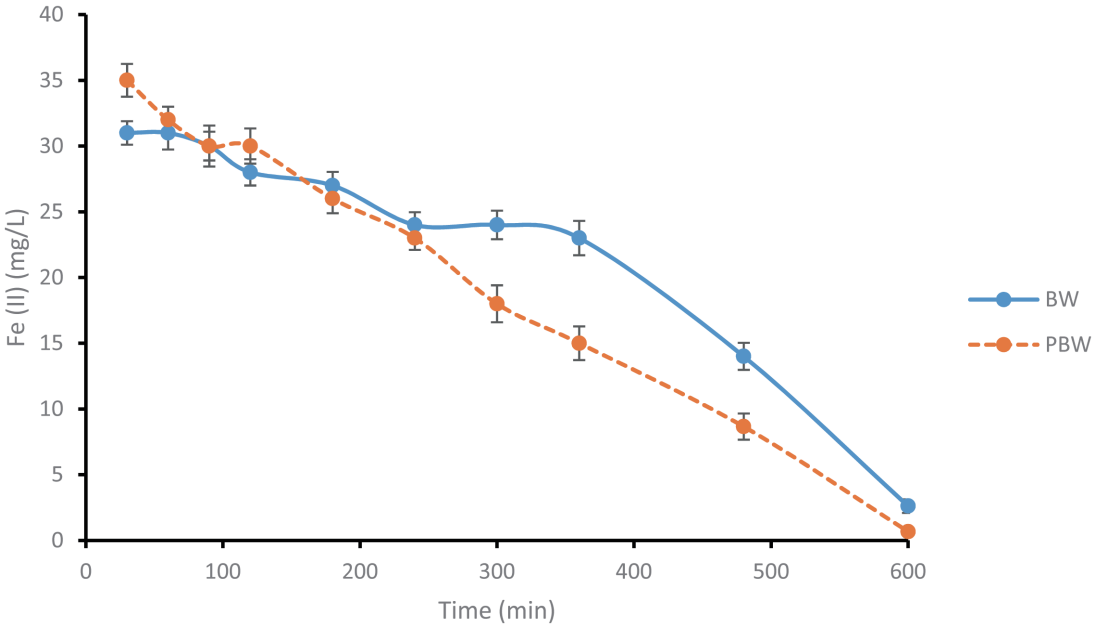

Fig. 5 Fe (II) biosorption over time on brewing waste (BW) and pre-treated brewing waste (PBW). [C_o = 40 mg L^{-1}, $pH_{initial}$ = 5 ± 0.2, 30 ˚C, 150 rpm, biosorbent dosage = 5 g L^{-1}]

Table 3 Summary of the kinetic model parameters for Fe (II) sorption on brewing waste.

Kinetic parameter	Biosorbents	
	BW	PBW
Pseudo first-order model		
k_1 (min^{-1})	7.00×10^{-4}	9.90×10^{-3}
q_e (mg g^{-1})	10.9	16.2
Pseudo second-order model		
k_2 (g mg^{-1} min^{-1})	2.90×10^{-3}	5.60×10^{-4}
q_e (mg g^{-1})	4.34	7.57
Elovich model		
γ (mg g^{-1} min^{-1})	1.96	2.60
a (mg g^{-1} min^{-1})	14.5	11.8
Intraparticle diffusion model		
k_{id} (mg g^{-1} $min^{-0.5}$)	0.095	0.283
Mass transfer model		
β_L (cm s^{-1})	1.38×10^{-5}	1.80×10^{-5}
S_S (cm^{-1})	208	286

[34], which reaffirms that the Fe (II) adsorption on brewing waste is heterogeneous to a great extent.

Proper understanding of mass transfer mechanisms would aid effective design of the adsorption system. The first portion with higher slope, often represent the external surface biosorption stage, the second stage corresponds to the gradual biosorption stage where intraparticle diffusion is rate controlling, and lastly, the third stage represents the equilibrium where the intraparticle diffusion slows down as a result of low solute concentration in the solution [22]. The intraparticle diffusion rate constants were calculated from the slope of the second phase of the plots of intraparticle diffusion of Fe (II) sorption on BW and PBW and are presented in **Table 3**. The intercept, which corresponds to the thickness

of the boundary layer was estimated as 1.889 mg g^{-1} and 0.82 mg g^{-1} for BW and PBW, respectively. This implies that surface sorption contributed more to the rate controlling step in BW than in PBW, as shown by previous study on biosorption of Fe (II) [20,34].

The values of mass transfer coefficients (β_L) derived from slope and intercept of the mass transfer plot for Fe (II) sorption on BW and PBW using equation (11) are presented in **Table 3**. The correlation coefficients were almost similar for both adsorbent; BW (R^2 = 0.936) and PBW (R^2 = 0.931). The mass transfer coefficients obtained shows that the rate of mass transfer from the work-solution to the brewing waste surface was quite fast, and thus cannot be considered as the rate limiting step. The deviation of some points on the plot from linearity indicates varying extent of mass transfer in the initial and final stages of the biosorption process [39].

CONCLUSION

Sorghum brewing waste was characterised to study its application in biosorption of Fe (II) in aqueous solution, for implementation in the remediation of surface water pollution in the vicinity of Potchefstroom. The study illustrates the importance of adsorption diffusion, reaction kinetics and mass transfer models in the sorption of Fe (II) on to the studied biosorbent. The specific surface area (mesopores) and total pore volume of the biosorbent improved with the acid pre-treatment. The acid pre-treated brewing waste was able to reduce the iron concentration to acceptable standard. The sorption isotherms based on correlation coefficient is best fitted with D-R model and Langmuir model for BW and PBW, respectively. The kinetic parameters fitted to five kinetic models were better described by pseudo-first-order and pseudo-second-order, as evident from the correlation coefficients. The mass transfer from the work-solution to the surface of the brewing waste particles was fast and cannot be rate limiting step. However, the intraparticle diffusion was very low and thus rate limiting step, and therefore controls the biosorption of Fe (II) in this study.

ACKNOWLEDGMENTS

This work is based on the research supported wholly by the National Research Foundation of South Africa (Grant Number: 111993). Any opinion, findings and conclusions or recommendations expressed are those of the authors, and NRF accepts no liability whatsoever in this regard.

REFERENCES

[1] Tibane E: Pocket guide to South Africa 2015/2016. South Africa: Government communication and information system, DMR; Report No. 978-0-620-72236-0, 2016.

[2] Manyatshe A, Fosso-Kankeu E, van der Berg D, Lemmer N, Waanders F, Tutu H: Dispersion of inorganic contaminants in surface water in the vicinity of Potchefstroom. *Phys. Chem. Earth Parts ABC*, **100**, 86–93, 2017. doi:10.1016/j.pce.2017.04.008

[3] SABS: South African National Standard Driking Water. South African Bureau of Standards, Pretoria, South Africa, 2005.

[4] WHO: Guidlines for Drinking Water quality. World Health Organization, Geneva, Switzerland, 2015.

[5] Richa J, Sonu K, Himanshu A, Kumar YA, Santosh K, Abhilasha M: Heavy metal bio-accumulating microbial isolates for remediation of metal contaminants from industrial effluents. *Int. J. Microbiol. Res.*, **9**(1), 837–841, 2017.

[6] Chojnacka K: Biosorption and bioaccumulation – the prospects for practical applications. *Environ. Int.*, **36**(3), 299–307, 2010. PMID:20051290 doi:10.1016/j.envint.2009.12.001

[7] Wang J, Chen C: Biosorbents for heavy metals removal and their future. *Biotechnol. Adv.*, **27**(2), 195–226, 2009. PMID:19103274 doi:10.1016/j.biotechadv.2008.11.002

[8] Coronado FF, Unciano NM, Cabacang RM, Hernandez JT: Removal of heavy metal compounds from industrial wastes using a novel locally-isolated *Vanrija* sp. HMAT2. *Philipp. J. Sci.*, **145**(4), 327–338, 2016.

[9] Jacob AA, Fidelis AE, Salaudeen KO, Queen KR: Sorghum: Most under-utilized grain of the semi-arid Africa. *Sch. J. Agric. Sci.*, **3**(4), 147–153, 2013.

[10] Musee N: Water and Wastewater Management in Sorghum Brewing Industry. Technical Report. Pretoria, South Africa: University of Pretoria, Department of Chemical Engineering UoP; 01/01/2017. Report No.: WRC Report No: TT 692/16, 2017.

[11] Okolo GN, Everson RC, Neomagus HWJP, Roberts MJ, Sakurovs R: Comparing the porosity and surface areas of coal as measured by gas adsorption, mercury intrusion and SAXS techniques. *Fuel*, **141**, 293–304, 2015. doi:10.1016/j.fuel.2014.10.046

[12] Ranjan D, Talat M, Hasan SH: Biosorption of arsenic from aqueous solution using agricultural residue 'rice polish'. *J. Hazard. Mater.*, **166**(2-3), 1050–1059, 2009. PMID:19131161 doi:10.1016/j.jhazmat.2008.12.013

[13] Rahman MS, Islam MR: Effects of pH on isotherms modeling for Cu(II) ions adsorption using maple wood sawdust. *Chem. Eng. J.*, **149**(1-3), 273–280, 2009. doi:10.1016/j.cej.2008.11.029

[14] Mahamadi C, Nharingo T: Utilization of water hyacinth weed (*Eichhornia crassipes*) for the removal of Pb(II), Cd(II) and Zn(II) from aquatic environments: an adsorption isotherm study. *Environ. Technol.*, **31**(11), 1221–1228, 2010. PMID:21046952 doi:10.1080/09593331003646604

[15] Igwe JC, Abia AA: Equilibrium sorption isotherm studies of Cd (II), Pb (II) and Zn (II) ions detoxification from waste water using unmodified and EDTA-modified maize husk. *Electron. J. Biotechnol.*, **10**(4), 536–548, 2007. doi:10.2225/vol10-issue4-fulltext-15

[16] Horsfall MJ, Spiff AI, Abia A: Studies on the influence of mercaptoacetic acid (MAA) modification of cassava (manihot sculenta cranz) waste biomass on the adsorption of Cu^{2+} and Cd^{2+} from aqueous solution. *Bull. Korean Chem. Soc.*, **25**(7), 969–976, 2004. doi:10.5012/bkcs.2004.25.7.969

[17] Abdel-Wahab O: Kinetic and isotherm studies of copper (II) removal from wastewater using various adsorbents. *Egypt. J. Aquat. Res.*, **33**(1), 125–143, 2007.

[18] Pokhrel D, Viraraghavan T: Arsenic removal from an aqueous solution by modified A. niger biomass: Batch kinetic and isotherm studies. *J. Hazard. Mater.*, **150**(3), 818–825, 2008. PMID:17582682 doi:10.1016/j.jhazmat.2007.05.041

[19] McKay G, Otterburn MS, Sweeney AG: Surface mass transfer processes during colour removal from effluent using silica. *Water Res.*, **15**(3), 327–331, 1981. doi:10.1016/0043-1354(81)90036-1

[20] Fontana IB, Peterson M, Cechinel MAP: Application of brewing waste as biosorbent for the removal of metallic ions present in groundwater and surface waters from coal regions. *J. Environ. Chem. Eng.*, **6**(1), 660–670, 2018. doi:10.1016/j.jece.2018.01.005

[21] Šillerová H, Komárek M, Chrastný V, Novák M, Vaněk A, Drábek O: Brewers draff as a new low-cost sorbent for chromium (VI): Comparison with other biosorbents. *J. Colloid Interface Sci.*, **396**, 227–233, 2013. PMID:23415478 doi:10.1016/j.jcis.2013.01.029

[22] Ferraz AI, Amorim C, Tavares T, Teixeira JA: Chromium(III) biosorption onto spent grains residual from brewing industry: equilibrium, kinetics and column studies. *Int. J. Environ. Sci. Technol.*, **12**(5), 1591–1602, 2015. doi:10.1007/s13762-014-0539-6

[23] Othman N, Asharuddin SM: *Cucumis melo* rind as biosorbent to remove Fe (II) and Mn (II) from synthetic groundwater solution. *Advanced Material Research*, **795**, 266–271, 2013. doi:10.4028/www.scientific.net/AMR.795.266

[24] Wu Y, Jiang L, Wen Y, Zhou J, Feng S: Biosorption of Basic Violet 5BN and Basic Green by waste brewery's yeast from single and multicomponent systems. *Environ. Sci. Pollut. Res. Int.*, **19**(2), 510–521, 2012. PMID:21833631 doi:10.1007/s11356-011-0577-2

[25] Ferraz E, Coroado J, Silva J, Gomes C, Rocha F: Manufacture of ceramic bricks using recycled brewing spent Kieselguhr. *Mater. Manuf. Process.*, **26**(10), 1319–1329, 2011. doi:10.1080/10426914.2011.551908

[26] Zhao Y, Wang D, Xie H, Won SW, Cui L, Wu G: Adsorption of Ag (I) from aqueous solution by waste yeast: kinetic, equilibrium and mechanism studies. *Bioprocess Biosyst. Eng.*, **38**(1), 69–77, 2015. PMID:24996651 doi:10.1007/s00449-014-1244-z

[27] Krishnarao RV, Subrahmanyam J, Jagadish Kumar T: Studies on the formation of black particles in rice husk silica ash. *J. Eur. Ceram. Soc.*, **21**(1), 99–104, 2001. doi:10.1016/S0955-2219(00)00170-9

[28] Adekola FA, Hodonou DSS, Adegoke HI: Thermodynamic and kinetic studies of biosorption of iron and manganese from aqueous medium using rice husk ash. *Appl. Water Sci.*, **6**(4), 319–330, 2016. doi:10.1007/s13201-014-0227-1

[29] Igwe J, Abia A: Adsorption kinetics and intraparticulate diffusivities for bioremediation of Co (II), Fe (II) and Cu (II) ions from waste water using modified and unmodified maize cob. *Int. J. Phys. Sci.*, **2**(5), 119–127, 2007.

[30] Shukla PM, Shukla SR: Biosorption of Cu(II), Pb(II), Ni(II), and Fe(II) on alkali treated coir fibers. *Sep. Sci. Technol.*, **48**(3), 421–428, 2013. doi:10.1080/01496395.2012.691933

[31] Shokoohi R, Saghi M, Ghafari H, Hadi M: Biosorption of iron from aqueous solution by dried biomass of activated sludge. *Iran. J. Environ. Health Sci. Eng.*, **6**(2), 107–114, 2009.

[32] Park JK, Choi SB: Metal recovery using immobilized cell suspension from a brewery. *Korean J. Chem. Eng.*, **19**(1), 68–74, 2002. doi:10.1007/BF02706876

[33] Srivastava VC, Swamy MM, Mall ID, Prasad B, Mishra IM: Adsorptive removal of phenol by bagasse fly ash and activated carbon: Equilibrium, kinetics and thermodynamics. *Colloids Surf. A Physicochem. Eng. Asp.*, **272**(1-2), 89–104, 2006. doi:10.1016/j.colsurfa.2005.07.016

[34] Kaveeshwar AR, Sanders M, Ponnusamy SK, Depan D, Subramaniam R: Chitosan as a biosorbent for adsorption of iron (II) from fracking wastewater. *Polym. Adv. Technol.*, **29**(2), 961–969, 2018. doi:10.1002/pat.4207

[35] Zhang Y, Zhao J, Jiang Z, Shan D, Lu Y: Biosorption of Fe (II) and Mn (II) ions from aqueous solution by rice husk ash. *Biomed. Res. Int.*, **2014**, 973095, 2014.

[36] Gadd GM: Biosorption: critical review of scientific rationale, environmental importance and significance for pollution treatment. *J. Chem. Technol. Biotechnol.*, **84**(1), 13–28, 2009. doi:10.1002/jctb.1999

[37] Sathasivam K, Haris MRHM: Banana trunk fibers as an efficient biosorbent for the removal of Cd (II), Cu (II), Fe (II) and Zn (II) from aqueous solutions. *J. Chil. Chem. Soc.*, **55**(2), 278–282, 2010. doi:10.4067/S0717-97072010000200030

[38] Adebayo GB, Mohammed AA, Sokoya SO: Biosorption of Fe (II) and Cd (II) ions from aqueous solution using a low cost adsorbent from orange peels. *J. Appl. Sci. Environ. Manag.*, **20**(3), 702–714, 2016. doi:10.4314/jasem.v20i3.25

[39] Acheampong MA, Pereira JPC, Meulepas RJW, Lens PNL: Kinetics modelling of Cu(II) biosorption on to coconut shell and *Moringa oleifera* seeds from tropical regions. *Environ. Technol.*, **33**(4), 409–417, 2012. PMID:22629612 doi:10.1080/09593330.2011.576705